A major purpose of the Technical Information Center is to provide the broadest dissemination possible of information contained in DOE's Research and Development Reports to business, industry, the academic community, and federal, state and local governments.

Although a small portion of this report is not reproducible, it is being made available to expedite the availability of information on the research discussed herein.

LA-UR -89-870

Los Alamos National Laboratory is operated by the University of California for the United States Department of Energy under contract W-7405-ENG-36

LA-UR--89-870

DE89 009359

TITLE Electron Temperature Measurements on FRX-C/LSM

AUTHOR(S) D. J. Rej

SUBMITTED TO 9th U.S. Compact Toroid Symposium
Alderbrook Inn Resort and Conference Center
Union, Washington
March 14-15, 1989

DISCLAIMER

Los Alamos Los Alamos National Laboratory
Los Alamos, New Mexico 87545

ELECTRON TEMPERATURE MEASUREMENTS ON FRX-C/LSM*

D. J. Rej

Los Alamos National Laboratory, Los Alamos NM 87545

I. **INTRODUCTION:** The electron temperature T_e has been measured with Thomson scattering in field-reversed configurations (FRCs) on the Los Alamos *FRX-C/LSM* experiment. FRCs formed and trapped *in-situ* in the θ-pinch source are studied. These experiments mark the first comprehensive FRC T_e measurements in over five years with data gathered on over 400 discharges.

Measurements are performed at a single point in space and time on each discharge. The Thomson scattering diagnostic consists of a Q-switched ruby laser focused from one end to a point 0.2 m from the axial midplane of the θ-pinch coil and at radius of either 0.00 or 0.10 m (*i.e.*, at the geometric axis or near the field null). Scattered light is collected, dispersed and detected with a 7-channel, triple-grating polychromator configured to detect light wavelengths between 658 and 692 nm. Photomultiplier currents are measured with gated A/D converters, with plasma background signals recorded 100-ns before and 100-ns after the laser pulse.

Electron temperatures are measured at either radial position during the time interval, $10 \le t \le 70$ μs, between FRC formation and the onset of the $n = 2$ instability which usually terminates the discharge. A variety of plasma conditions have been produced by adjusting three external parameters: (1) the initial deuterium fill pressure p_0; (2) the reversed bias magnetic field B_b; and (3) the external magnetic field B_w. The fill-pressure scan has been performed at $B_b \approx 60$ mT and $B_w \approx 0.4$ T (at time $t = 30$ μs) with p_0 set at either 2, 3, 4 or 5 mtorr. The bias-field scan, $37 \le B_b \le 95$ mT, has been performed at $p_0 = 3$ mtorr and $B_w \approx 0.4$ T. There are also limited data at $p_0 = 5$ mtorr and large bias, $B_b = 100$ mT, a condition where in earlier experiments, a soft x-ray diagnostic revealed large flute-like distortions of the plasma column.[1] B_w is adjusted by changing the capacitance of the main θ-pinch bank. At $p_0 = 3$ mtorr and $B_b \approx 65$ mT, B_w has been increased from 0.4 T to 0.6 T.

II. **OBSERVATIONS:** The average electron temperature ranges from 90 to 190 eV, depending on plasma conditions and the measurement radius. Both the shot-to-shot variation and the measurement error are typically 10% to 20%. To within this variation, the T_e remains constant in time (*e.g.*, see Fig. 1), similar to that observed on *FRX-B*[2] and *FRX-C*.[3]

An interesting range of plasma conditions has been produced with the bias field scan (*cf.* Table I). In particular, at $p_0 = 3$ mtorr and $B_w \approx 0.4$ T, the inferred trapped flux ϕ_p increases from 1.0 to 7.5 mWb when B_b is increased from 37 to 95 mT. The average FRC parameters quoted in Table I are for time $t = 30$ μs, except for the confinement times (obtained with the 0-D model[4]) which are time and shot averaged. When the bias field is increased, the electron temperature near the field null increases, almost proportional with the plasma separatrix radius r_s as illustrated by the data in Fig. 2.

There is a weak dependence on the fill pressure. As p_0 is increased, with B_b and B_w constant, colder, higher-density FRCs are produced without much change in the separatrix radius (see Table II). For the conditions $p_0 \le 4$ mtorr, relatively long-lived FRCs are produced. $T_e(r \approx R)$ decreases by 15% as p_0 is increased from 2 to 4 mtorr. $T_e(r = 0)$, on the other hand, remains constant at about 133 eV.

At 5-mtorr, the plasma decays away so rapidly that one may question whether or not an FRC equilibrium is ever attained. The electron temperature at low bias is quoted in Table II, while at high bias we observe 118 eV at $r = 0$ and 128 eV at $r \approx R$.

The FRC has been compared to the linear θ-pinch configuration. With the reversed bias field removed, open field line plasmas have been generated at 3 and 4 mtorr. A plasma column with excluded flux radius of 0.1 m is observed to form and rapidly decay, typically in 30 μs. When compared to FRCs, colder temperatures, $T_e(r=0) = 85 \pm 10$ eV, are observed.

There is also a weak dependence on the external field B_w. The changes to FRC parameters that result from a 40% increase in B_w are listed in Table III. In general, the higher-field plasmas are smaller, more dense, hotter, contain less flux, and have poorer confinement. The density and pressure-balance temperature are observed to increase as expected from adiabatic scaling[5] $n \sim B_w^{6/5}$, $T \sim B_w^{4/5}$. The electron temperature shows a more modest 10 to 15% increase with B_w, values less than the standard deviations (20%) and the predictions from adiabatic compression theory (27%).

III. **DISCUSSION:** As previously observed with smaller FRCs,[2,3] the electron temperature at the geometric axis is consistently 8% to 24% lower than at the field null. Under the usual assumption that T_e is constant on a flux surface [in particular, $T_e(0) \simeq T_e(r_s)$], these data suggest the existence of a flat $T_e(r)$ profile inside the separatrix. A flat profile in an FRC usually implies anomalous electron energy loss. A time-independent temperature can be explained by loss terms in the electron energy equation which are of equal magnitude to the heating input, *i.e.*,

$$(3/2)N(dT_e/dt) = P_{in} - P_e - NT_e/\tau_N = 0 \quad , \qquad (1)$$

where N is the FRC electron inventory, and P_{in} is the total input power to these electrons from coulomb collisions with the ions, adiabatic compression, and resistive dissipation. P_e represents the "non-convective" losses due to all processes other than particle diffusion. The NT_e/τ_N term in Eq. 1 estimates the cooling due to particle diffusion in which every lost electron removes the energy $(5/2)T_e$. P_{in} is estimated at 40 to 100 MW, corresponding to a local heating rate of 2 to 4 eV/μs. From Eq. 1, we estimate the non-convective losses to range between 20 and 50 MW which is 20 to 30% of the total plasma power loss P_T. Particle diffusion still dominates the energy confinement. For 2 and 3 mtorr conditions, both P_{in} and P_T are about 2-times lower than that inferred at $p_o = 5$ mtorr on *FRX-C*.[3] Despite the improvement in the electron energy confinement, losses remain anomalous. Cross-field electron thermal conduction is often thought to be principally responsible for P_e. Simulations with the 1¼-D transport code[6] indicate that a perpendicular electron thermal conductivity of 35-times classical is necessary to explain the 3-mtorr condition of Table II.

There is no obvious correlation between confinement and electron temperature. In particular, there is no apparent change in τ_ϕ even though the classical scaling factor $R^2T_e^{3/2}$ could be varied by more than a factor of 5 in the 3-mtorr bias scan. For the rigid-rotor equilibrium, the inferred field-null resistivity varies between 8 and 100-times the classical value with $Z_{eff} = 1$ (see Fig. 3a). The same data have been compared to a theory based on anomalous resistivities from low-frequency drift instabilities[7] (see Fig. 3b). While there is agreement in magnitude, there is no clear correlation with the theoretical scaling factor $r_s^2B_w/T_e(1 + T_e/T_i)^{1/2}$, which on *FRX-C/LSM*, could be varied by over a factor of 2.

*FRC research at Los Alamos is funded by the USDOE.

[1]R. E. Siemon *et al.*, Proc. 12th IAEA Conf., Nice (1988) paper CN-50/C-4-1.
[2]W. T. Armstrong *et al.*, *Phys Fluids* **24**, 2068 (1981).
[3]D. J. Rej and W. T. Armstrong, *Nucl. Fusion* **24**, 177 (1984).
[4]R. E. Chrien, private communication.
[5]R. L. Spencer, M. Tuszewski, and R. K. Linford, *Phys Fluids* **26**, 1564 (1983).
[6]H.-Y. Hsiao, K. A. Werley, K.-M. Ling, Los Alamos National Lab Report *LA 11212 MS* (1988)
[7]N. A. Krall, Preprint *KA-89-01* (to be published)

TABLE I: Average FRX-C/LSM parameters vs. bias field obtained during the Thomson scattering data run. Error bars denote shot-to-shot standard deviations.

PARAMETER	UNITS	low bias	medium bias	high bias
bias field	mT	44 ± 5	65 ± 3	86 ± 2
fill pressure	mtorr	2.99 ± 0.01	3.04 ± 0.0	3.03 ± 0.03
PI timing	μsec	18.5 ± 0.1	18.6 ± 0.1	18.7 ± 0.1
B_w	T	0.39 ± 0.01	0.41 ± 0.02	0.41 ± 0.01
r_s	mm	111 ± 9	154 ± 9	186 ± 6
V_s	liter	59 ± 9	107 ± 10	143 ± 8
ϕ_p	mWb	1.1 ± 0.4	3.5 ± 0.7	6.3 ± 0.8
$\langle n \rangle$	$10^{20} m^{-3}$	9.3 ± 0.6	7.2 ± 0.6	6.0 ± 0.5
$T_e + T_i$	eV	443 ± 28	521 ± 31	582 ± 34
$T_e(r=R)$	eV	135 ± 6	162 ± 29	186 ± 36
$T_e(r=0)$	eV	103 ± 17	145 ± 22	143 ± 14
τ_ϕ	μsec	131 ± 72	160 ± 34	122 ± 48
τ_E	μsec	41 ± 10	82 ± 14	69 ± 17
τ_N	μsec	105 ± 24	185 ± 53	181 ± 107

TABLE II: Average FRX-C/LSM parameters vs. fill pressure obtained during the Thomson scattering data run.

PARAMETER	UNITS	2 mtorr	3 mtorr	4 mtorr	5 mtorr
fill pressure	mtorr	2.09 ± 0.06	3.04 ± 0.05	4.05 ± 0.06	4.98 ± 0.04
bias field	mT	58 ± 3	53 ± 5	57 ± 4	71 ± 3
PI timing	μsec	19.2 ± 0.1	18.6 ± 0.1	13.9 ± 0.2	13.9 ± 0.1
B_w	T	0.44 ± 0.01	0.41 ± 0.02	0.45 ± 0.01	0.40 ± 0.01
r_s	mm	160 ± 5	151 ± 12	167 ± 5	156 ± 15
V_s	liter	87 ± 6	104 ± 13	115 ± 17	118 ± 16
ϕ_p	mWb	4.2 ± 0.4	3.4 ± 0.8	5.0 ± 0.4	3.7 ± 1.1
$\langle n \rangle$	$10^{20} m^{-3}$	6.4 ± 0.4	7.4 ± 0.6	10.5 ± 0.8	11.1 ± 1.1
$T_e + T_i$	eV	670 ± 40	516 ± 34	431 ± 27	328 ± 27
$T_e(r=R)$	eV	165 ± 15	156 ± 28	140 ± 14	142 ± 15
$T_e(r=0)$	eV	133 ± 24	135 ± 26	128 ± 20	117 ± 18
τ_ϕ	μsec	128 ± 53	158 ± 36	117 ± 31	25 ± 5
τ_E	μsec	54 ± 11	78 ± 15	77 ± 13	23 ± 5
τ_N	μsec	149 ± 101	173 ± 50	160 ± 79	40 ± 15

TABLE III: Average FRX-C/LSM parameters vs. external B-field obtained during the Thomson scattering data run.

PARAMETER	UNITS	low field	high field
B_w @ 30 μs	T	0.41 ± 0.02	0.57 ± 0.04
bias field	mT	65 ± 3	65 ± 3
fill pressure	mtorr	3.04 ± 0.05	3.05 ± 0.05
PI timing	μsec	18.7 ± 0.1	18.6 ± 0.1
r_s	mm	154 ± 9	130 ± 8
V_s	liter	107 ± 11	69 ± 8
ϕ_p	mWb	3.5 ± 0.7	2.8 ± 0.5
$\langle n \rangle$	$10^{20} m^{-3}$	7.2 ± 0.5	10.6 ± 0.9
$T_e + T_i$	eV	522 ± 29	704 ± 55
$T_e (r=R)$	eV	155 ± 27[a]	170 ± 30[c]
$T_e (r=0)$	eV	135 ± 25[b]	155 ± 32[d]
τ_ϕ	μsec	160 ± 34	122 ± 40
τ_I	μsec	82 ± 14	57 ± 7
τ_N	μsec	181 ± 43	122 ± 24

[a] $B_w(t=30\,\mu s) = 0.40 \pm 0.01$ T [b] $B_w = 0.41 \pm 0.01$ T [c] $B_w = 0.54 \pm 0.02$ T [d] $B_w = 0.58 \pm 0.01$ T

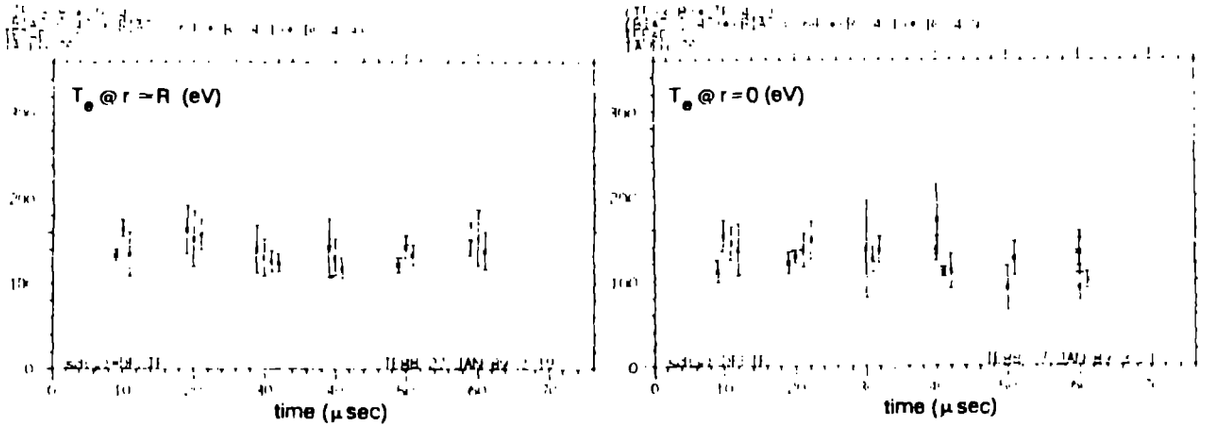

Fig. 1: Electron temperatures near the field null and at the geometric axis plotted vs time for the 4-mtorr conditions of Table II. Each data point represents a separate discharge while the error bars are from the Gaussian fits.

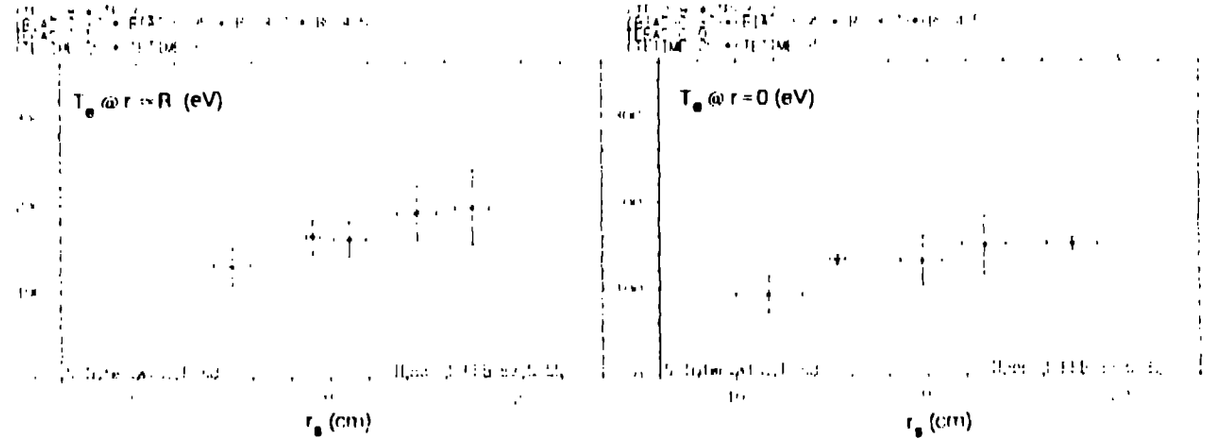

Fig. 2: Electron temperatures near the field null and at the geometric axis at time t = 30 μ sec, plotted vs the plasma separatrix radius obtained during the bias field scan (cf. Table I). Each data point represents an average of several shots while the error bars denote standard deviations.

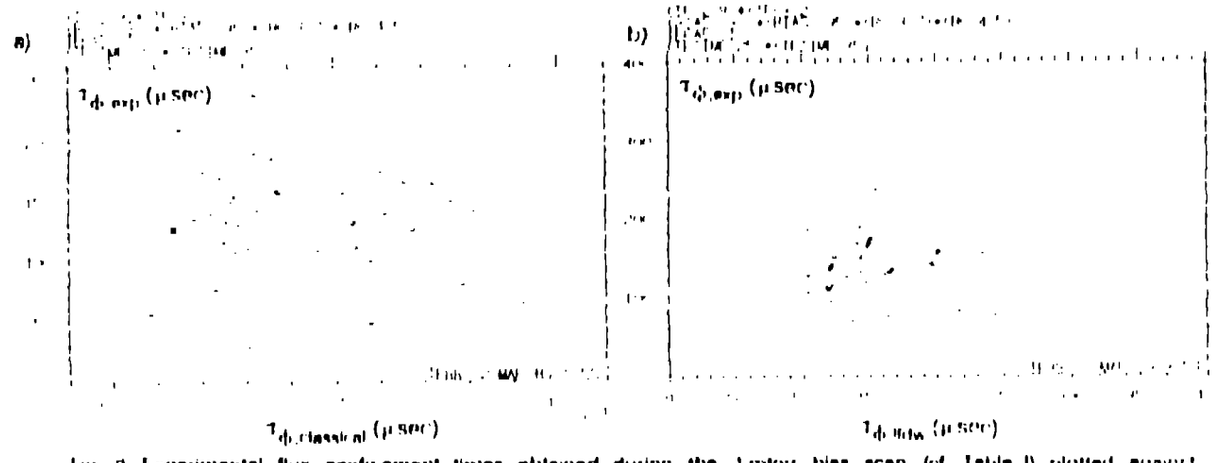

Fig. 3 Experimental flux confinement times obtained during the 3 mtorr bias scan (cf. Table I) plotted against theoretically predicted times with (a) classical resistivity and (b) anomalous resistivity due to low frequency drift instabilities. Each data point represents a separate discharge.